

# V<sub>1</sub>-situated Stalk Subunits of the Yeast Vacuolar Proton-translocating ATPase\*

(Received for publication, May 30, 1997, and in revised form, July 29, 1997)

John J. Tomashek‡, Laurie A. Graham§, Maria U. Hutchins‡, Tom H. Stevens§, and Daniel J. Klionsky‡¶

From the ‡Section of Microbiology, University of California, Davis, California 95616 and the §Institute of Molecular Biology, University of Oregon, Eugene, Oregon 97403

**The proton-translocating ATPase of the yeast vacuole is an enzyme complex consisting of a large peripheral membrane sector (V<sub>1</sub>) and an integral membrane sector (V<sub>0</sub>), each composed of multiple subunits. The V<sub>1</sub> sector contains subunits that hydrolyze ATP, whereas the V<sub>0</sub> sector contains subunits that translocate protons across the membrane. Additional subunits in both sectors couple these activities. Here we have continued our examination of intermediate subunits primarily associated with the V<sub>1</sub> but also implicated in interactions with the V<sub>0</sub>. Interactions between Vma7p (F) and Vma8p (D) and between Vma4p (E) and Vma10p (G) are described. Although Vma7p and Vma10p have been observed to interact with the V<sub>0</sub> sector, our results indicate that these subunits behave primarily as canonical V<sub>1</sub> sector subunits. We categorize these four subunits as “stalk” subunits to distinguish them from the known catalytic (A and B) and proton-translocating (c, c', and Vma16p) subunits and to highlight their intermediate nature. Furthermore, we show that the *in vivo* stability of Vma4p is dependent upon interaction with Vma10p. This may be important in the regulation of assembly, since these two subunits add to the V<sub>1</sub> during later stages of V<sub>1</sub> assembly. This is the first demonstration of interdependence between ATPase subunits for structural stability.**

The vacuolar proton-translocating ATPases are a family of organellar proton pumps found throughout the endomembrane system of eukaryotic cells. The V-ATPases<sup>1</sup> are related to the F-type ATP synthases of mitochondria, chloroplasts, and bacterial membranes. The enzymes of both families have similar subunit stoichiometries (1), similar structures based on electron micrographic imaging (2, 3), and similar mechanisms (4). Furthermore, the major catalytic subunits (A and B in the V-type;  $\beta$  and  $\alpha$  in the F-type) show primary sequence homology of about 30%, whereas the principal proton-translocating subunits, the c subunits or proteolipids, also show high sequence homology (5–7). The intermediate peripheral sector subunits and the remaining integral sector subunits show little or no homology between the two families. This suggests an overall

conservation of gross structure with a low tolerance for deviation at the sites mediating the two principal activities: ATP hydrolysis (or synthesis) and proton translocation. In contrast, the intermediate subunits that couple these activities have greater evolutionary flexibility.

The subunits coupling the F<sub>1</sub> peripheral sector to the F<sub>0</sub> membrane sector,  $\gamma$ ,  $\delta$ ,  $\epsilon$ , and the hydrophilic portion of F<sub>0</sub>-b, are described as “core” or “stalk” subunits because they reside in the midst of the catalytic subunits and appear to bridge physically the two sectors as seen in electron micrographic images. The subunits presumably bridging the V<sub>1</sub> and V<sub>0</sub> sectors, C (Vma5p), D (Vma8p), E (Vma4p), F (Vma7p), G (Vma10p), H (Vma13p), d (Vma6p), and perhaps hydrophilic portions of Vph1p, can therefore also be thought of as stalk or core subunits of the V-ATPase.

We have identified a hierarchy of V<sub>1</sub> subcomplexes which assemble in the cytoplasm of yeast strains deleted for individual subunits (Tables I and II; Ref. 8). Significant among these subcomplexes is complex II (A<sub>3</sub>B<sub>3</sub>DEFG), the soluble cytosolic form of the V<sub>1</sub> complex. Smaller subcomplexes assemble to form complex II when combined *in vitro*, indicating they are bona fide intermediates of assembly (9). Here we further analyze subunits Vma7p (F) and Vma10p (G), which were not extensively examined previously. These subunits are intriguing because they seem to associate with both the V<sub>1</sub> and V<sub>0</sub> sectors. Vma7p is required for assembly of V<sub>0</sub>, although it otherwise behaves as a V<sub>1</sub> subunit (10). Vma10p was originally reported as an hydrophilic subunit tightly associated with the V<sub>0</sub> (11), similar to Vma6p (12). Here we demonstrate that Vma10p behaves predominantly as a canonical V<sub>1</sub> subunit. Nonetheless, Vma10p also has homology to the hydrophilic portion of the F<sub>0</sub>-b subunit, suggesting it may be in close association with V<sub>0</sub> subunits within the holoenzyme (13).

## MATERIALS AND METHODS

**Reagents, Antibodies, and Strains**—All reagents were from Sigma unless stated otherwise. HEPES buffer was from Research Organics, Inc. Media components were from Difco. For native gels, the W303-based *vma10*Δ strains were used, a gift from Nathan Nelson (Tel Aviv University). Construction of the *vma10*Δ strain for subcellular fractionation, nitrate stripping, and glycerol gradient analysis was done as follows. A *vma10*Δ disruption fragment was generated by PCR amplification using oligonucleotides (5'-TTTTTTCATTGTTGCTCAGAAC-TATGTAATATTCTCTTTATTGTACTGAGAGTGCACCAT-3', and 5'-AAAAGATATATGATTAGAAAAGTGAATGTAATGCAATACTGTGCGGTTATTCACACCGC-3') with 39 bp of sequence complementary to the 5'- and 3'-flanking sequence of *VMA10* and 21 bp complementary to the sequence flanking the auxotrophic markers in the pRS series of yeast shuttle vectors (14, 15). The genomic locus of *VMA10* was disrupted by the method of Rothstein (16). Yeast haploid strain, SF838-1D (*Mata ura3-52 leu2-3, 112 his4-519 ade6 pep4-3*), was transformed using the lithium acetate method with the PCR-generated *vma10*Δ:LEU2 disruption fragment (17) to generate strain LGY14. Disruption was confirmed by immunoblot analysis using antibodies specific for Vma10p.

\* This work was supported by National Institutes of Health Public Service Grants GM53396 (to D. J. K.) and GM38006 (to T. H. S.). The costs of publication of this article were defrayed in part by the payment of page charges. This article must therefore be hereby marked “advertisement” in accordance with 18 U.S.C. Section 1734 solely to indicate this fact.

¶ To whom correspondence should be addressed. Tel.: 916-752-0277; Fax: 916-752-9014.

<sup>1</sup> The abbreviations used are: V-ATPase, vacuolar proton-translocating adenosine triphosphatase; DSP, dithiobis(succinimidyl propionate); PAGE, polyacrylamide gel electrophoresis; PVDF, polyvinylidene difluoride; bp, base pair(s); PCR, polymerase chain reaction; MES, 4-morpholineethanesulfonic acid; MOPS, 4-morpholinepropanesulfonic acid.

TABLE I  
Gene and monomer designations for ATPase subunits discussed in this paper

Subunit	Yeast gene	Approximate molecular mass kDa
A	VMA1	69
B	VMA2	60
C	VMA5	42
D	VMA8	32
E	VMA4	27
F	VMA7	14
G	VMA10	13
H	VMA13	54
d	VMA6	36
(None)	VPH1	100

TABLE II  
Subcomplexes of the V-ATPase

Complexes are defined by their position on a native gel, starting at the top with complex I, and counting down the length of the gel. Molecular masses were calculated by the method of Hedrick and Smith as previously described (8). Subunits define those subunits detected in each complex; this list is not exhaustive, as all subunits have not been examined. The column titled "In strains" describes the yeast strains in which the complex in question is detected. Stoichiometry is estimated from the mass of the complex, its known composition in subunits, and the known stoichiometry of the complete enzyme. Complexes III and VI are described in this study.

Complex	Mass	Subunits	In strains	Stoichiometry
I	ND <sup>a</sup>	Vma1p, Vma2p, Vma4p, Vma8p, Vma10p	<i>vma7Δ</i>	A <sub>3</sub> B <sub>3</sub> DEG
II (V <sub>1</sub> )	576 ± 97	Vma1p, Vma2p, Vma4p, Vma7p, Vma8p, Vma10p	Wild-type, <i>vma3Δ</i> , <i>vma5Δ</i>	A <sub>3</sub> B <sub>3</sub> DEFG
III	96 ± 28	Vma4p, Vma10p	All but <i>vma4Δ</i> , <i>vma10Δ</i>	E <sub>2</sub> G <sub>2</sub>
IV	317 ± 49	Vma1p, Vma2p, Vma7p, Vma8p	<i>vma4Δ</i> , <i>vma10Δ</i>	A <sub>2</sub> B <sub>2</sub> DF
V	156 ± 49	Vma2p	<i>vma4Δ</i> , <i>vma10Δ</i>	B?
VI	ND	Vma7p, Vma8p	All but <i>vma7Δ</i> , <i>vma8Δ</i>	DF

All antibodies except those to Vma7p and Vma10p have been described previously. For Vma7p, two oligonucleotides, 5'-CTAAATCA-GATCTGAGAAACGTACTCTTCTTATAGC-3' and 5'-GTTTTGGTCTA-GAGAATTCGCTTACTCACC-3', were used in PCR to generate a 384-bp fragment including the entire VMA7 ORF minus the initial methionine and introducing a 5' *Bgl*II restriction site and a 3' *Xba*I site (underlined) that were used to subclone the fragment into *Bam*HI- and *Xba*I-digested pMAL-c2 vector (New England Biolabs) to generate pLG27. *Escherichia coli* cells carrying the plasmid were induced for protein expression by the addition of 1 mM isopropyl-1-thio-β-D-galactopyranoside. A 56-kDa maltose-binding protein-Vma7p fusion protein was isolated from *E. coli* cell extracts using amylose resin according to the provided protocol and used to inject New Zealand White rabbits. For Vma10p, two oligonucleotides, 5'-GGAAGATCTTCCCAAAAAACG-GAATTGCC-3' and 5'-GCTCTAGAGAATTCCAAGGCATTGATATGG-3', were used to PCR-amplify a 1300-bp fragment containing the entire VMA10 open reading frame after the initial methionine. The primers introduce unique *Bgl*II and *Eco*RI restriction sites, respectively (underlined), used to subclone the PCR fragment into *Bam*HI- and *Eco*RI-digested pGEX2T (Pharmacia Biotech Inc.) to yield pLG46. Addition of isopropyl-1-thio-β-D-galactopyranoside to *E. coli* cultures carrying pLG46 induces the synthesis of a 41-kDa glutathione S-transferase-Vma10p fusion protein that was purified and used to inject New Zealand White rabbits.

**Native Gel Electrophoresis**—Native gels were run, blotted, and probed as described previously (8). Briefly, pre-run 6-cm 6% acrylamide gels were loaded and run for 100 min at 150 V and 4 °C in a continuous HEPES/imidazole buffer system (pH 7.4). Proteins were electroblotted onto PVDF membranes, autoclaved, blocked, and probed with antibodies as indicated in the figures.

**Subcellular Fractionation, Nitrate Stripping, and Glycerol Gradient Analysis**—Whole cell extracts were prepared from wild-type (SF838-1D), *vma2Δ* (SF838-1D::vma2), *vma3Δ* (SF838-1D::vma3), and *vma10Δ*

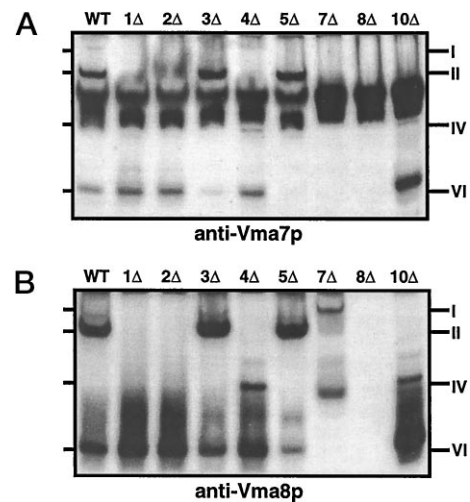


FIG. 1. Vma7p and Vma8p form a subcomplex of the V-ATPase. Extracts were prepared by lysis of yeast spheroplasts with native sample buffer (10 mM Tris-acetate, 5 mM potassium acetate, 1 mM EDTA, 10% glycerol, 0.05% each bromophenol blue and xylene cyanol) to a final protein concentration of 1 mg/ml. 10 μl of each was run on a 6% polyacrylamide gel, pH 7.4, for 100 min at a constant 150 V. The gel was electroblotted to PVDF and probed with antisera to Vma7p (A) and to Vma8p (B). The positions of V<sub>1</sub> subcomplexes (see Table I) are indicated on the right.

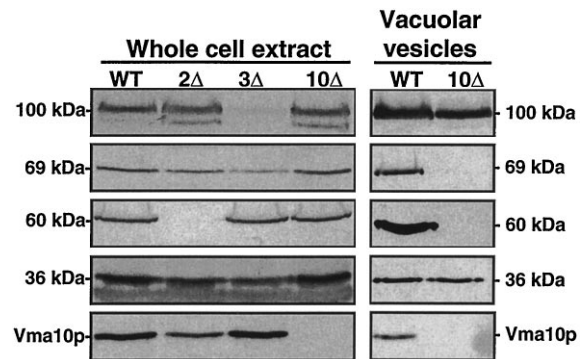


FIG. 2. Fate of V<sub>0</sub> and V<sub>1</sub> subunits in wild-type and *vmaΔ* strains. Detection of V-ATPase subunits by immunoblot analysis. 30 μg of whole cell extract proteins or 5 μg of vacuolar membrane proteins were separated by electrophoresis, and immunoblots were probed with either monoclonal antibodies specific for the 100-, 69-, or 60-kDa proteins or polyclonal antibodies against the 36-kDa protein or Vma10p.

as described (18). Vacuolar membranes were isolated from wild-type and *vma10Δ::LEU2* cells (LGY14) as described previously (19). Wild-type vacuolar membranes were treated with potassium nitrate in the presence or absence of 5 mM ATP as described previously (20). For glycerol gradient fractionation, vacuolar membranes were isolated from SF838-1D wild-type cells and washed three times with 10 mM Tris, pH 7.4, 1 mM EDTA as described (19). 500 μg of vacuolar membranes were solubilized with 2% zwitterionic detergent ZW3-14 (Calbiochem) and separated by centrifugation through a 20–50% glycerol density gradient at 174,000 × g for 20 h using a Beckman SW41 rotor (20). Fractions were collected (750 μl), and proteins were precipitated with 5% trichloroacetic acid (final concentration) and separated by SDS-PAGE. SDS-polyacrylamide gel electrophoresis and immunoblot analysis were performed as described previously (12). Immunoblots were probed with antibodies against the 100-, 60-, and 36-kDa V-ATPase subunits and polyclonal antibodies against Vma10p, as indicated in the figures. Proteins were visualized by chemiluminescence (NEN Life Science Products) after incubation with horseradish peroxidase-conjugated secondary antibody (Amersham).

**Cross-linking**—Spheroplasts were prepared as described previously (8). These were lysed in phosphate-buffered saline (10 mM Na<sub>2</sub>PO<sub>4</sub>, 1.8 mM KH<sub>2</sub>PO<sub>4</sub>, 137 mM NaCl, 2.7 mM KCl, pH 7.2) for an estimated protein concentration of 1 mg/ml. Large membranes and unlysed cells were removed by brief high speed microcentrifugation. A 1% volume of

DSP (100 mM in dimethyl sulfoxide) was added for a final concentration of 1 mM and allowed to react on ice for 90 min. The reaction was quenched with the addition of Tris-HCl (pH 8.0) to a final concentration of 100 mM. Samples of the cross-linked reactions were combined 1:1 with 2 × Laemmli buffer without β-mercaptoethanol and resolved by 12% SDS-PAGE. Lanes from this gel were cut out, soaked in 1 × Laemmli with β-mercaptoethanol, and then loaded sideways onto the stack of a 15% SDS-PAGE gel. These were transferred to PVDF and probed with antibodies as described in the figures.

**Labeling and Immunoprecipitation**—Yeast strains were grown to ~0.8 A<sub>600</sub> in SMD buffered to pH 5.5 (50 mM MES, 50 mM MOPS). Cells were harvested (10 ml) and resuspended in 200 μl of SMD, pH 5.5. Expre<sup>35S</sup>S label (NEN Life Science Products) was added in two equal aliquots during the first 5 min for a final concentration of 0.5 μCi/μl and incubated at 30 °C for 15 min total. Unlabeled methionine/cysteine (0.4 mM and 0.2 mM, final concentrations, respectively) in SMD pH 5.5 and 0.2% yeast extract was added to chase. Samples were removed at the indicated times and precipitated with trichloroacetic acid (10% final concentration) and incubated on ice. After two 1-ml acetone washes of the trichloroacetic acid pellet, samples were resuspended in 100 μl of MES-urea resuspension buffer (50 mM sodium phosphate, 50 mM MES, pH 7.0, 1% SDS, 0.5% 2-mercaptoethanol, 1 mM sodium azide) and resuspended by vigorous vortexing with acid-washed glass beads. Supernatant fractions were immunoprecipitated twice with antisera as indicated in the figures. Immunoprecipitation has been described previously (21). Immunoprecipitated proteins were resolved on 10% SDS-PAGE and quantitated on a Molecular Dynamics STORM PhosphorImager.

## RESULTS

**Vma7p Forms Complexes with Vma8p**—The F subunit of the V-ATPase, Vma7p in yeast, interacts with both V<sub>1</sub> and V<sub>0</sub> sectors. It is necessary for V<sub>0</sub> assembly, suggesting it may interact directly with the membrane sector (10). At the same

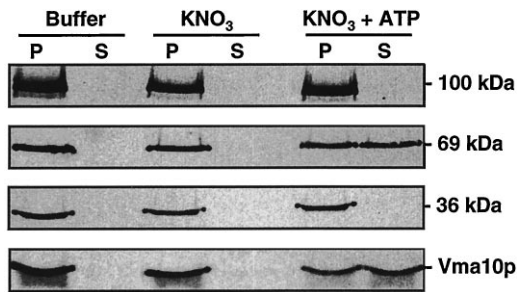
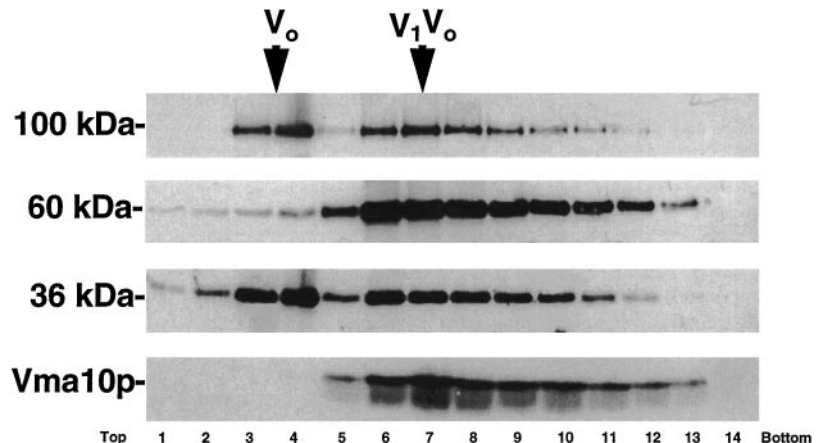


**FIG. 3. Nitrate stripping of V<sub>1</sub> subunits from wild-type membranes.** Freshly prepared vacuolar membranes were resuspended in either buffer, 100 mM KNO<sub>3</sub> or 100 mM KNO<sub>3</sub> plus 5 mM ATP. Samples were incubated for 30 min at 37 °C, then centrifuged 15 min at 50,000 × *g* to generate pellet (P) and supernatant (S) fractions. Proteins in supernatant were precipitated by the addition of trichloroacetic acid (5% final concentration). Membrane and supernatant fractions from 5 μg of vacuolar membranes were separated by SDS-PAGE and probed using antibodies specific for the 100-, 69-, and 36-kDa proteins and Vma10p.

**FIG. 4. Glycerol gradient fractionation of Vma10p.** 500 μg of vacuolar membranes from wild-type cells were solubilized with 2% ZW3-14 and separated by centrifugation through a 12-ml 20–50% glycerol density gradient. 750-μl fractions were collected, and proteins were trichloroacetic acid-precipitated (5% final concentration) and separated by SDS-PAGE. Immunoblots were probed with antibodies against the 100-, 60-, and 36-kDa V-ATPase subunits and Vma10p. Arrows indicate the positions in the gradient of the V<sub>0</sub> sector and the assembled V-ATPase (V<sub>1</sub>V<sub>0</sub>).



time, Vma7p can be stripped from the membrane with nitrate (10) and is a component of cytosolic complexes seen on native gels (8). Its role in the formation of V<sub>1</sub> and how it modulates V<sub>0</sub> assembly are not known.

Previously, we used an epitope-tagged version of Vma7p to show its presence in cytosolic complexes II (A<sub>3</sub>B<sub>3</sub>DEFG) and IV (A<sub>2</sub>B<sub>2</sub>DF) on native gels (8). Using a new antibody raised against Vma7p itself, we probed native blots of extracts from a library of *vmaΔ* deletion strains (Fig. 1A). For comparison, we probed an identical blot with antibodies against Vma8p (Fig. 1B). The presence of these subunits in both complexes II and IV was confirmed, although Vma7p in complex IV (in the *vma4Δ* and *vma10Δ* extracts) is just barely visible beneath a large band which we believe is nonspecific due to its appearance in the *vma7Δ* strain. We also observed a lower band (designated complex VI in Fig. 1) absent in the *vma7Δ* and *vma8Δ* strains. Additionally, an uncharacterized form of Vma8p, possibly a free or oligomeric form of the subunit, runs just below the position of complex IV in *vma7Δ*.

Steady-state levels of complex VI are *vma* mutation-dependent, and the levels of both Vma7p and Vma8p are affected proportionally, suggesting they have a constant stoichiometry in this complex in all strains (Fig. 1). In *vma3Δ* and *vma5Δ*, the signal for Vma7p in complex VI is barely visible, although it can be seen after long exposure (data not shown). Complex VI appears to be in equilibria with larger complexes containing Vma7p and Vma8p, such as IV and II. The *vma1Δ* and *vma2Δ* strains do not influence the mobility of the Vma7p and Vma8p bands, suggesting that Vma1p and Vma2p are not part of complex VI. Also, like complex III (subunits E and G; see below) and complex II, complex VI is found in wild-type cells, indicating it is not merely an artifact found in mutant strains.

**Vma10p Behaves as a V<sub>1</sub> Subunit**—Like VMA7, the yeast VMA10 gene encodes a small (13-kDa; subunit G) hydrophilic protein that copurifies with the V-ATPase and is required for its function (11). Cold inactivation studies on the yeast V-ATPase (11) indicated that Vma10p remained associated with the vacuolar membrane fraction while canonical V<sub>1</sub> subunits, e.g. Vma1p and Vma4p, were released. Thus the subunit was initially assigned to the V<sub>0</sub> sector of the V-ATPase. However, under the experimental conditions used by these researchers, the hydrophilic subunit Vma6p, a known subunit of the V<sub>0</sub> sector, was also released from the membranes, indicating that these conditions released both known V<sub>0</sub> and V<sub>1</sub> subunits. The homologous protein from the *Manduca sexta* V-ATPase (37% identical) fractionates with the V<sub>1</sub> complex and can be stripped from membranes using both cold inactivation and treatment with a chaotropic reagent similar to the behavior of other V<sub>1</sub> subunits (22, 23). Also, the mammalian V-ATPase equivalent to Vma10p, subunit G, fractionates with the V<sub>1</sub>

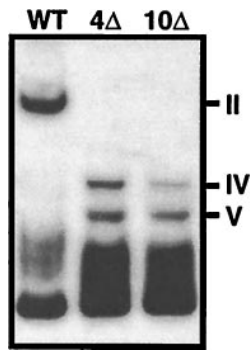


FIG. 5. **Native gel analysis of *vma10Δ*.** Extracts from wild-type (WT), *vma4Δ*, and *vma10Δ* strains were prepared, run on native PAGE, and immunoblotted as described in Fig. 1, except antibodies to Vma2p were used for this blot. The positions of V<sub>1</sub> subcomplexes are indicated on the right.

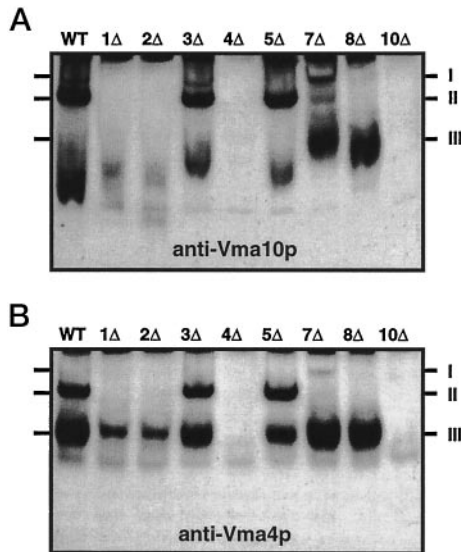


FIG. 6. **Native gel analysis of Vma10p in wild-type and *vmaΔ* strains.** Immunoblots were prepared as described in Fig. 1, except that they were probed with antibodies to Vma10p (A) and antibodies to Vma4p (B). The positions of V<sub>1</sub> subcomplexes (see text) are indicated on the right.

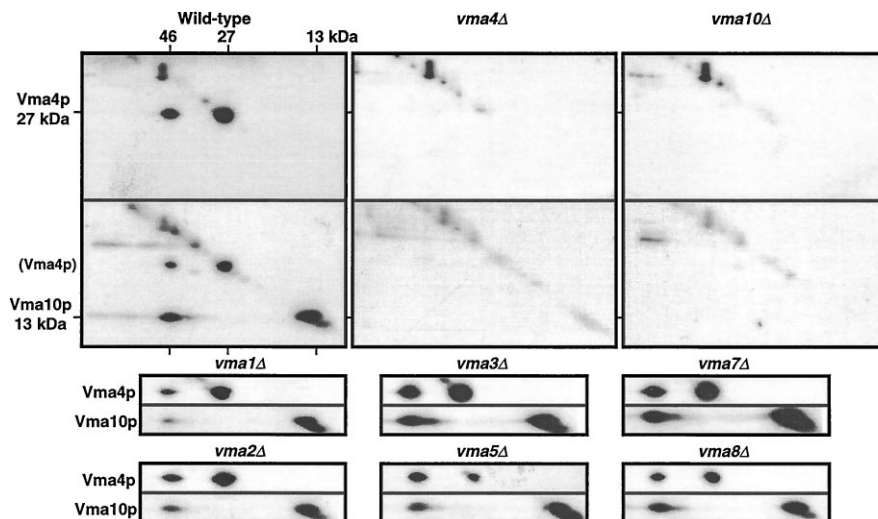


FIG. 7. **Cross-linking of Vma4p and Vma10p.** Yeast of the strains indicated were converted to spheroplasts and lysed with phosphate-buffered saline (see "Materials and Methods"). DSP in dimethyl sulfoxide was added in 1% of the total volume to a final concentration of 1 mM, and the mixture was incubated on ice for 1 h. The reaction was terminated by the addition of Tris-HCl, pH 8.0, to a final concentration of 100 mM. Samples were diluted in 2 × Laemmli buffer without β-mercaptoethanol and separated in the first dimension (left to right) on a 12% SDS-PAGE. These were cut into strips, soaked in Laemmli with β-mercaptoethanol for 1 h at 37 °C, and then laid sideways onto the stack of a 15% SDS-PAGE slab gel and separated in the second dimension (down). The gel was blotted onto PVDF and probed first with antibodies to Vma4p, then stripped and reprobed with antibodies to Vma10p. Incomplete stripping from the first blot results in residual signal from Vma4p. Positions of the subunits in the second dimension are indicated on the right. Molecular mass of subunits and cross-link products in the first dimension are indicated above.

sector and stimulates the ATPase activity of V<sub>1</sub> (24).

The discrepancies between yeast and other systems led us to examine further the role of Vma10p in the yeast V-ATPase complex, and this has revised our view on the sector assignment for this subunit. Previous studies indicated that the stability of bona fide V<sub>0</sub> subunits are interdependent, since the loss of any one V<sub>0</sub> subunit results in the decreased steady-state level of the 100-kDa V<sub>0</sub> subunit due to the rapid degradation of unassembled V<sub>0</sub> subunits (12, 25). Immunoblot analyses of whole cell extracts and vacuolar vesicles prepared from wild-type and *vmaΔ* mutant strains are shown in Fig. 2. Whole cell extracts prepared from yeast cells lacking a V<sub>1</sub> subunit (*vma2Δ*) and a *vma10Δ* deletion strain had the same level of 100-kDa protein as extracts from wild-type yeast cells. Only yeast cells lacking a V<sub>0</sub> subunit (*vma3Δ*) showed reduced steady-state levels of the 100-kDa subunit. Vacuolar membrane preparations from *vma10Δ* cells revealed wild-type levels of the 100-kDa polypeptide present on the vacuolar membrane. It is evident that, in the absence of Vma10p, the V<sub>0</sub> subunits are stable and targeted to the vacuole consistent with Vma10p being a V<sub>1</sub> subunit. As with all *vma* deletion strains (except *vma13Δ* (26)), the V<sub>1</sub> subunits fail to associate with the vacuolar membrane in *vma10Δ* mutant cells (12).

*Vma10p Is Stripped from Membranes with Nitrate*—Although Vma10p was not released from the membrane by cold inactivation (11), we tested whether it would be stripped from wild-type vacuolar membranes with the chaotropic reagent nitrate in the presence of ATP. Using antibodies specific for each subunit we examined the fractionation profile of both V<sub>1</sub> and V<sub>0</sub> subunits. When vacuolar membranes were treated with potassium nitrate alone, all V-ATPase subunits remained associated with the membrane pellet (P). Treatment of membranes with nitrate and ATP caused the release of V<sub>1</sub> subunits such as the A subunit (Vma1p, 69 kDa) as shown in Fig. 3. The integral membrane 100-kDa V<sub>0</sub> subunit (Vph1p) is not released by this treatment nor is the hydrophilic subunit Vma6p, which has been shown to be tightly associated with, and necessary for the assembly of, the V<sub>0</sub> sector (12). Vma10p was released from the membranes by this treatment, indicating that it is a V<sub>1</sub> subunit. We have determined the fractionation profile of all

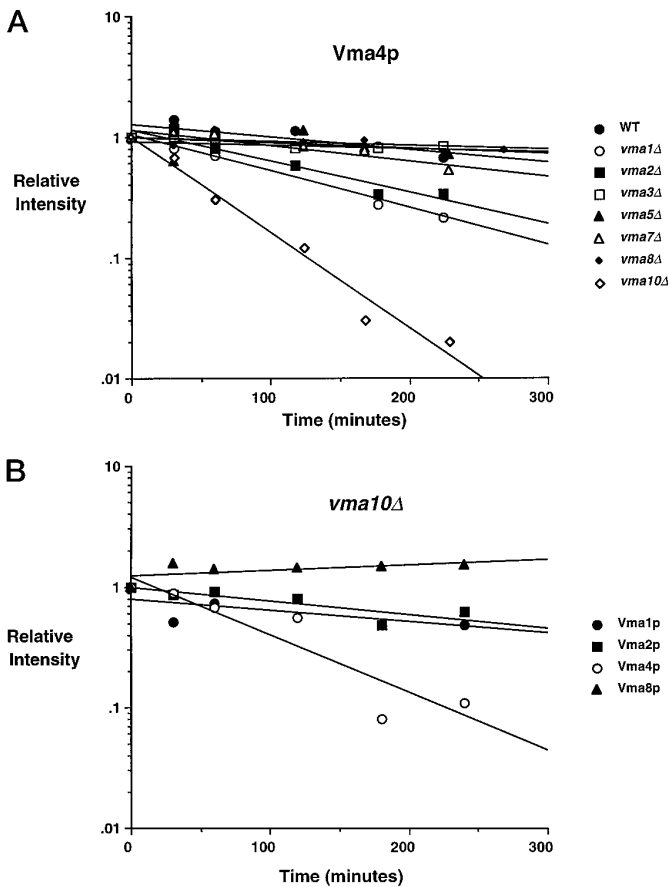


FIG. 8. **Subunit-dependent degradation of Vma4p.** Strains indicated were pulse-labeled for 15 min with Expre<sup>35</sup>S<sup>35</sup>S-label and chased with excess methionine/cysteine. Samples were taken at the time points indicated and precipitated with trichloroacetic acid. Vma subunits were immunoprecipitated as described under "Materials and Methods." *A*, precipitation of Vma4p from different *vmaΔ* strains. *B*, precipitation of subunits from *vma10Δ*. Signals were quantitated on Molecular Dynamics Storm 840 PhosphorImager. Values were normalized to the zero time point, and lines were fitted with Cricket Graph software.

V-ATPase subunits (except the proteolipids Vma3p, Vma11p, and Vma16p) and have found that of all the subunits examined only the 100-kDa and 36-kDa  $V_0$  subunits remain tightly associated with the membrane after treatment with nitrate and ATP (data not shown).

**Vma10p Does Not Sediment with  $V_0$  on Glycerol Density Gradients**—We have observed that while both  $V_1$  and  $V_0$  subunits fractionate with the intact V-ATPase complex,  $V_0$  subunits also sediment together to a position of lower molecular mass when detergent-solubilized vacuolar membranes are separated on a glycerol density gradient (27).  $V_1$  subunits, such as the B subunit (Vma2p, 60 kDa), fractionate to a single peak possessing maximum ATPase activity (Fig. 4). A biphasic profile is observed for the 100-kDa and 36-kDa  $V_0$  subunits, with one peak coincident with the  $V_1$  subunits representing fully assembled V-ATPase. A second, lighter peak is observed containing only  $V_0$  proteins representing  $V_0$  subcomplexes present on vacuolar membranes. Vma10p fractionates only with the fully assembled V-ATPase complex and is not found in the fractions where the  $V_0$  sector occurs alone. Taken together, the genetic and biochemical data indicate that Vma10p is a  $V_1$  subunit.

**Vma10p Shows Behavioral Similarities to Vma4p in Native Gels**—Deletions of  $V_1$  subunits can result in the formation of subcomplexes of the peripheral sector (8, 28). Fig. 5 shows the results from a native gel analysis of extracts from wild-type,

*vma4Δ*, and *vma10Δ* strains of yeast, revealing that Vma10p is required for assembly of complex II. These data further support the assignment of Vma10p to the  $V_1$  sector. Also, the band pattern seen for the *vma10Δ* strain appears nearly identical to that of the *vma4Δ* strain, distinguished by the presence of complexes IV and V, hitherto unique to the *vma4Δ* strain (see also Fig. 1). Complex IV was previously characterized as a large subcomplex lacking Vma4p. Apparently Vma10p is also absent from this complex. This native gel profile further suggests Vma4p and Vma10p might interact to form complex III.

To identify complexes containing Vma10p, antibodies were prepared against peptides and used to probe native blots of extracts from our collection of *vmaΔ* mutants (Fig. 6A). An identical blot was probed with antibodies against Vma4p for comparison (Fig. 6B). Vma10p is present in complexes I and II, indicating that it is a component of the soluble  $V_1$ . Vma10p appears to run at the same position as complex III in the *vma7Δ* and *vma8Δ* strains, suggesting that it is a subunit of this complex. In other strains, however, it runs as a smear below the position of complex III. These migration patterns are *vmaΔ* mutant-specific, *i.e.* while they differ between deletion strains, they are consistent from extract to extract prepared from the same strain. Smearing may be due to associations with other proteins, lipids, or nucleic acids. Because the native gel is pH 7.4 and Vma10p has a pI  $\sim$ 9, it must be associated with other molecules to move into the gel at all.

**Vma10p Cross-links to Vma4p**—The odd behavior of Vma10p in the native gel demanded an alternate approach. We examined the proximity of Vma4p and Vma10p by cross-linking experiments, treating extracts from wild-type and deletion strains with the reducible cross-linker DSP, followed by two-dimensional (non-reducing 1° followed by reducing 2°) gel electrophoresis and immunoblot analysis. A substantial fraction of both Vma4p and Vma10p travel together off the diagonal (Fig. 7), indicating they can be cross-linked to a significant degree in extracts from all strains except their cognate deletion strains. The cross-linked product has a molecular mass of approximately 46 kDa, allowing for one of each subunit (27-kDa E subunit and 13-kDa G subunit, respectively) in the linkage product. This suggests that these subunits interact specifically and independently of other subunits or complexes. The calculated mass of complex III is  $96 \pm 28$  kDa, twice that of the cross-linked product, suggesting complex III may be a tetramer ( $E_2G_2$ ) as previously proposed (8). Examination of the same membranes with antibodies to Vma2p and Vma8p indicated that these subunits did not undergo any significant cross-linking to other subunits under our conditions (data not shown). These data further support the idea that the Vma4p-Vma10p interaction is close and specific. Like complex VI, complex III is present not only in mutant cells, but in the wild-type strain as well.

**Stability of Vma4p Is Affected by Vma10p**—In general, the steady-state levels of individual  $V_1$  subunits are relatively unaffected by deletions of other  $V_1$  or  $V_0$  subunits (18, 28). We observed, however, that the steady-state level of Vma4p was greatly diminished in the *vma10Δ* strain (Fig. 7; data not shown). We performed a pulse-chase analysis of subunit degradation in wild-type and deletion strains (Fig. 8). Vma4p is strongly destabilized in the absence of Vma10p (Fig. 8A) with a half-life of  $\sim$ 1 h. It is slightly destabilized in the absence of Vma1p or Vma2p, where it has a half-life on the order of about 2 h. In other strains the half-life of Vma4p is greater than 4 h. This correlates to the steady-state levels of complex III observed in these strains. Other  $V_1$  subunits (Vma1p, Vma2p, and Vma8p) do not show such variable levels of stability in the absence of Vma10p (Fig. 8B). Thus, the *in vivo* stability of

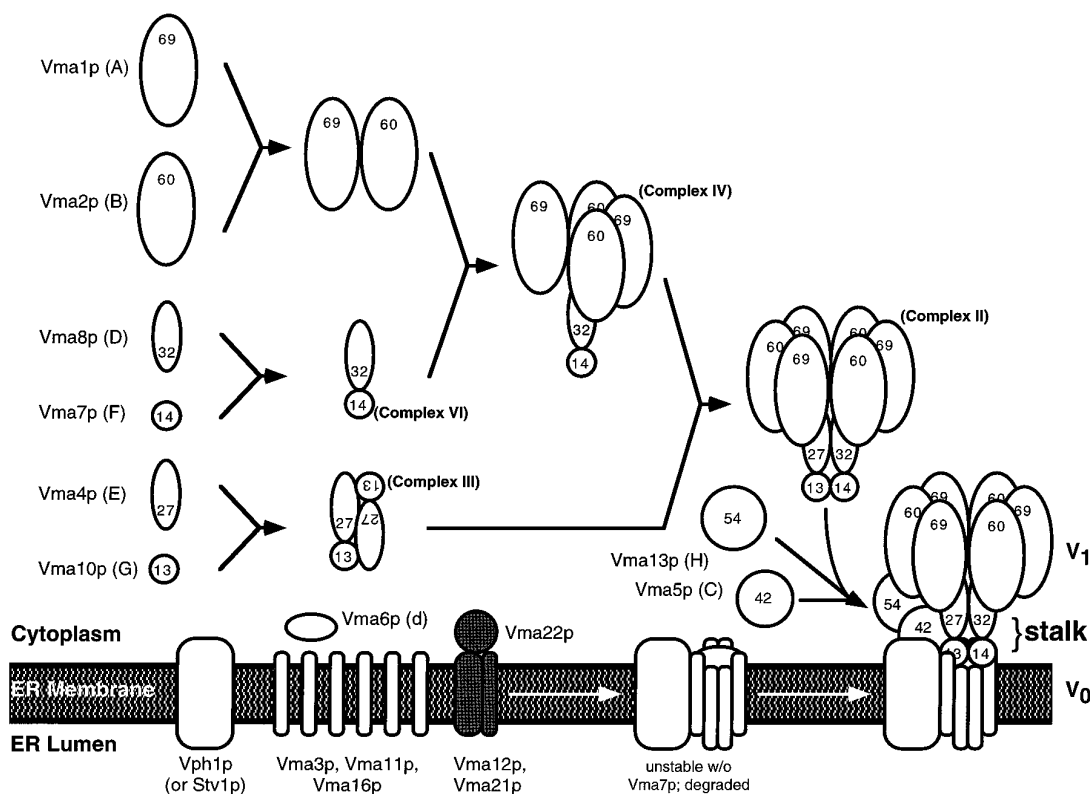


FIG. 9. **Convergent assembly of the yeast vacuolar ATPase.** Individual subunits interact to form subcomplexes. These subsequently assemble into the cytosolic  $V_1$  complex. Subunits of the enzyme itself are *white with black outline*;  $V_1$  subunits are labeled with their apparent molecular mass (in kDa). Subunits in *gray* are accessory proteins necessary for assembly of  $V_0$ , but which are not part of the final enzyme structure. See text for further explanation.

Vma4p is highly dependent on other subunits, especially Vma10p.

#### DISCUSSION

The subunits Vma4p (E), Vma7p (F), Vma8p (D), and Vma10p (G) are unique to the V-ATPase class of proton pumps. While subunits A (Vma1p) and B (Vma2p) show significant sequence homology to the  $\beta$  and  $\alpha$  subunits, respectively, of the F-type ATPases, the  $\gamma$ ,  $\delta$ , and  $\epsilon$  subunits which comprise the core/stalk region of the  $F_1$  enzyme and attach and couple it to the  $F_0$  have no sequence homologs yet identified among the V-type enzymes (5–7). However, because these enzymes are structurally and functionally similar, it is reasonable to assume there is some structural and functional homolog to the stalk region of the F-type pump in the V-ATPase.

There is an heuristic value to thinking of the subunits Vma4p, Vma7p, Vma8p, and Vma10p (as well as Vma5p, Vma6p, and Vma13p, perhaps) as couplers between the catalytic and proton pumping subunits of the enzyme.  $V_1$  can assemble to a high degree in the cytosol, although in wild-type cells the assembly of the two sectors may not be separate and discrete; subcomplexes of each sector may associate before either sector is complete. Peripheral subunits capable of interacting with  $V_0$  components might do so at early stages of  $V_1$  assembly, although these early  $V_1$ - $V_0$  interactions are not obligatory for assembly of either sector alone or subsequent assembly of the complete enzyme. The dependence of  $V_0$  stability on the presence of Vma7p establishes a link between the catalytic and proton translocating sectors. Proposals that Vma4p (29), Vma8p (30), or both (8) could have functional homology to the  $\gamma$  subunit of the F-type enzyme reinforce a similar theme.

Fig. 9 shows our model for the V-ATPase in the context of its assembly from separate sectors. The final structure focuses on

the position of subunits discussed here. Vma4p and Vma8p serve as structure/function homologs of the  $\gamma$  subunit; thus they are shown emerging from the core of the  $V_1$  sector. Vma7p and Vma10p interact with Vma8p and Vma4p, respectively, and although both are clearly components of the  $V_1$  sector, they may each interact with the  $V_0$  sector. These are key components of the stalk region, and these subunits interact to form partial complexes, specifically complexes III and VI, prior to incorporation into the  $V_1$  sector. The product of *VMA5* (Vma5p, the C subunit) and *VMA13* (Vma13p, (26)) may also be involved with interactions between the  $V_1$  and  $V_0$  sectors. Subunits C and E (Vma4p) of the bovine clathrin-coated vesicle can be co-immunoprecipitated (31), and these subunits can be cross-linked to subunit D (Vma8p) and the proteolipid (subunit c, Vma3p, Vma11p, and/or Vma16p) (32). We also have data indicating that Vma5p is involved in glucose-mediated disassembly of  $V_1$  and  $V_0$  (33).<sup>2</sup>

Complex VI exhibits consistent behavior. The steady-state levels of Vma7p and Vma8p in complex VI parallel each other as they vary among different *vma* $\Delta$  mutant strains, suggesting a constant stoichiometry between these subunits within this complex. The level of the complex itself varies in relationship to the formation of larger complexes, with less complex VI present when complex II can be formed, suggesting an equilibrium between these forms *in vivo*. Accumulation of complex VI in some deletion strains appears to be due to an inability to assemble further.

Complex III is mercurial. This complex depends upon both Vma4p and Vma10p (Fig. 6B, lane 9). On native gels, Vma10p occasionally runs at the position of complex III (Fig. 6A, lanes 7 and 8), but in some strains the position of complex III (as

<sup>2</sup> J. Tomashek, unpublished data.

defined by the position of Vma4p; Fig. 6B) appears to be independent of the position of Vma10p. As reported previously, the steady-state level of complex III is affected by the absence of Vma1p and Vma2p (Fig. 6B, lanes 2 and 3, and Ref. 8), although neither subunit is found in complex III. However, the dependence of complex III on Vma10p appears to be much more absolute than its dependence on either Vma1p or Vma2p, and Vma4p and Vma10p cross-link to each other with high efficiency in all strains in which they are present. No significant cross-linking to other subunits (Vma2p and Vma8p) was observed (data not shown).

The dependence of Vma4p stability on the presence of other subunits raises interesting possibilities in terms of the regulation of assembly. Complex III and its components are the first  $V_1$  subunits found to be sensitive to the presence or absence of other subunits. Since complex III appears to be a late addition to the complete sector, regulation of this complex may control the level of membrane-competent  $V_1$  sector available for assembly into the complete enzyme. *VMA4* is also unusual in that it has two putative TUF binding sites in its 5' region, approximately 250 bp upstream of the initiation codon. These sites have been implicated in the transcriptional regulation of this subunit. Hence, availability of this subunit appears to be tightly controlled at all levels of biosynthesis. Regulation of the ATPase through control of  $V_1$  assembly may be a significant control mechanism *in vivo*, and this mechanism may be independent of regulation by the equilibrium between separate  $V_1$  and  $V_0$  sectors and the complete holoenzyme.

*Acknowledgments*—We thank Dr. Nathan Nelson for the gift of the W303-based *vma* $\Delta$  strains used for the native gel and cross-linking studies. We would also like to thank Dr. Sidney Scott for critical help with the manuscript.

## REFERENCES

1. Arai, H., Terres, G., Pink, S., and Forgac, M. (1988) *J. Biol. Chem.* **263**, 8796–8802
2. Bowman, B. J., Dschida, W. J., Harris, T., and Bowman, E. J. (1989) *J. Biol. Chem.* **264**, 15606–15612
3. Bowman, B. J., Dschida, W. J., and Bowman, E. J. (1992) *J. Exp. Biol.* **172**, 57–66
4. Kasho, V. N., and Boyer, P. D. (1989) *Proc. Natl. Acad. Sci. U. S. A.* **86**, 8708–8711
5. Mandel, M., Moriyama, Y., Hulmes, J. D., Pan, Y. C., Nelson, H., and Nelson, N. (1988) *Proc. Natl. Acad. Sci. U. S. A.* **85**, 5521–5524
6. Gogarten, J. P., Kibak, H., Dittrich, P., Tai, L., Bowman, E. J., Bowman, B. J., Manolson, M. F., Poole, R. J., Date, T., Oshima, T., Konishi, J., Denda, K., and Yoshida, M. (1989) *Proc. Natl. Acad. Sci. U. S. A.* **86**, 6661–6665
7. Nelson, H., and Nelson, N. (1989) *FEBS Lett.* **247**, 147–153
8. Tomashek, J. J., Sonnenburg, J. L., Artimovich, J. A., and Klionsky, D. J. (1996) *J. Biol. Chem.* **271**, 10397–10404
9. Tomashek, J. J., Garrison, B. S., and Klionsky, D. J. (1997) *J. Biol. Chem.* **272**, 16618–16623
10. Graham, L. A., Hill, K. J., and Stevens, T. H. (1994) *J. Biol. Chem.* **269**, 25974–25977
11. Supekova, L., Supek, F., and Nelson, N. (1995) *J. Biol. Chem.* **270**, 13726–13732
12. Bauerle, C., Ho, M. N., Lindorfer, M. A., and Stevens, T. H. (1993) *J. Biol. Chem.* **268**, 12749–12757
13. Supekova, L., Sbia, M., Supek, F., Ma, Y., and Nelson, N. (1996) *J. Exp. Biol.* **199**, 1147–1156
14. Sikorski, R. S., and Hieter, P. (1989) *Genetics* **122**, 19–27
15. Lorenz, M. C., Muir, R. S., Lim, E., McElver, J., Weber, S. C., and Heitman, J. (1995) *Gene* **158**, 113–117
16. Rothstein, R. J. (1983) *Methods Enzymol.* **101**, 202–211
17. Ito, H., Fukuda, Y., Murata, K., and Kimura, A. (1983) *J. Bacteriol.* **153**, 163–168
18. Kane, P. M., Kuehn, M. C., Howald-Stevenson, I., and Stevens, T. H. (1992) *J. Biol. Chem.* **267**, 447–454
19. Roberts, C. J., Raymond, C. K., Yamashiro, C. T., and Stevens, T. H. (1991) *Methods Enzymol.* **194**, 644–661
20. Kane, P. M., Yamashiro, C. T., and Stevens, T. H. (1989) *J. Biol. Chem.* **264**, 19236–19244
21. Klionsky, D. J., Cueva, R., and Yaver, D. S. (1992) *J. Cell Biol.* **119**, 287–299
22. Graf, R., Harvey, W. R., and Wiczorek, H. (1996) *J. Biol. Chem.* **271**, 20908–20913
23. Lepier, A., Graf, R., Azuma, M., Merzendorfer, H., Harvey, W. R., and Wiczorek, H. (1996) *J. Biol. Chem.* **271**, 8502–8508
24. Crider, B. P., Andersen, P., White, A. E., Zhou, Z., Li, X., Mattsson, J. P., Lundberg, L., Keeling, D. J., Xie, X.-S., Stone, D. K., and Peng, S.-B. (1997) *J. Biol. Chem.* **272**, 10721–10728
25. Hirata, R., Graham, L. A., Takatsuki, A., Stevens, T. H., and Anraku, Y. (1997) *J. Biol. Chem.* **272**, 4795–4803
26. Ho, M. N., Hirata, R., Umemoto, N., Ohya, Y., Takatsuki, A., Stevens, T. H., and Anraku, Y. (1993) *J. Biol. Chem.* **268**, 18286–18292
27. Graham, L. A., Hill, K. J., and Stevens, T. H. (1995) *J. Biol. Chem.* **270**, 15037–15044
28. Doherty, R. D., and Kane, P. M. (1993) *J. Biol. Chem.* **268**, 16845–16851
29. Bowman, E. J., Steinhart, A., and Bowman, B. J. (1995) *Biochim. Biophys. Acta* **1237**, 95–98
30. Nelson, H., Mandiyan, S., and Nelson, N. (1995) *Proc. Natl. Acad. Sci. U. S. A.* **92**, 497–501
31. Puopolo, K., Sczekan, M., Magner, R., and Forgac, M. (1992) *J. Biol. Chem.* **267**, 5171–5176
32. Adachi, I., Puopolo, K., Marquez-Sterling, N., Arai, H., and Forgac, M. (1990) *J. Biol. Chem.* **265**, 967–973
33. Kane, P. M. (1995) *J. Biol. Chem.* **270**, 17025–17032